Macromolecules

COMMUNICATION TO THE EDITOR

pubs.acs.org/Macromolecules

A New Strategy to Microporous Polymers: Knitting Rigid Aromatic Building Blocks by External Cross-Linker

Buyi Li,[†] Ruini Gong,[†] Wei Wang,[‡] Xin Huang,[†] Wang Zhang,[†] Huanmin Li,[†] Chunxiao Hu,[†] and Bien Tan[†,*]

[†]School of Chemistry and Chemical Engineering, Huazhong University of Science and Technology, Wuhan, 430074, China

[‡]State Key Laboratory of Applied Organic Chemistry, College of Chemistry and Chemical Engineering, Lanzhou University, Lanzhou 730000, China

Supporting Information

ABSTRACT: A series of microporous polymers has been obtained via a low-cost versatile strategy, which involves "knitting" rigid aromatic building blocks, such as benzene, biphenyl, 1,3,5-triphenylbenzene, methylbenzene, chlorobenzene, and phenol using an external cross-linker. These materials are predominantly microporous and exhibit high surface areas. Moreover, different building blocks can generate materials with different pore structures, functional groups and application properties, which are significant for materials design.

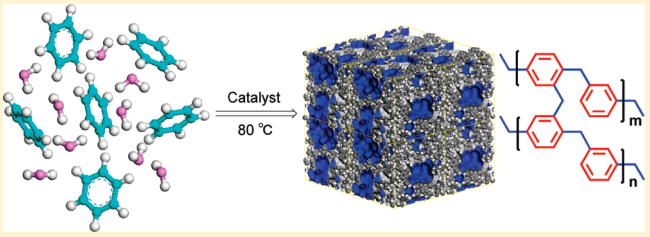

The porous materials with extraordinarily high surface area have attracted enormous scientific attention due to their diverse potential applications in separation,[1] heterogeneous catalysis,[2] and gas storage.[3] During the last few decades, the surge to develop such useful materials has led scientists to produce a number of novel porous materials such as metal organic frameworks (MOFs),[4] covalent organic frameworks (COFs),[5] porous organic cages,[6] and microporous organic polymers (MOPs),[7] in addition to traditional porous materials such as zeolites and activated carbon etc. Among these porous materials, MOPs have attracted a particular attention due to their unique properties such as large surface area, low skeletal density and high chemical stability. "Davankov resins", that is, styrene-type polymers hypercrosslinked by Friedel−Crafts reaction,[8] are one of the earliest types of MOPs and have been studied extensively, coming into industrial practice at the end of 1990s, however, the releasing hydrogen halide as byproduct is detrimental and hard to tackle.[3d,9] Hyper-cross-linked polypyrrole or polyaminobenzene or aminobenzene represent another kind of pioneering MOPs.[10] These two synthesis method can only be adapted to very limited monomers. Very recently, various other new kinds of MOPs have been developed, based on several types of reaction, such as polymers of intrinsic microporosity (PIMs) with dioxane unit,[3b] microporous polymers such as conjugated microporous polymers (CMPs)[11] and porous aromatic frameworks (PAFs)[12] by various cross-coupling reactions of aromatic compound. MOPs were also formed by trimerizations of ethynyl[13] or nitrile groups,[14] by amide or imide or imine formation,[15] and via "click" chemistry.[16] All of these approaches have aimed to develop new microporous organic materials with higher surface areas and controlled pore sizes and functions. However, the transition metal catalysts or noble metal catalysts used for synthesis of CMPs, PAFs, and some other MOPs are expensive and rare. It is often also complicated to synthesize the monomers which must bear halogen,[11a] ethynyl[17] or stereocontrolled structures such as spirocyclic monomers[17,18] used in MOPs. Hence, the sustainable mass production of MOPs is an unanswered challenge.

In this report, we propose a new strategy, which involves "knitting" rigid building blocks with an external cross-linker. We used a simple one-step Friedel−Crafts reaction of a low-cost cross-linker with ordinary, low functionality aromatic compounds to produce cost-effective microporous polymers with very high surface areas and the only byproduct was methanol. In this one-step cross-linking approach, formaldehyde dimethyl acetal (FDA) was used as an external cross-linker to react with various aromatic monomers (Scheme 1, parts a−c). Typically, the monomer (e.g., benzene, 0.02 mol, 1.56 g), cross-linker (FDA, 0.06 mol, 4.56 g) and the catalyst ($FeCl_3$, 0.06 mol, 9.75 g) were dissolved in 1,2-dichloroethane (DCE, 20 mL) and heated at 45 °C for 5 h to form a network, and then heated at 80 °C for 19 h to complete the condensation reaction and to produce a microporous polymer (yield = ∼95%). After washing the resulting solid product with methanol several times, until the filtrate liquor was nearly colorless, the product was Soxhlet extracted in methanol for 24 h followed by drying in a vacuum oven at 60 °C for 24 h. For different monomers, the ratio of external cross-linker was adjusted because of differing numbers of crossliking functionalities and different reactivities. All samples were obtained as light or dark brown powders. The SEM and TEM micrographs indicated the formation of amorphous nanosize particles in samples **1**−**5** (particles smaller than 100 nm; Figures S1−S5, Supporting Information). The formation of spherical

Received: March 19, 2011
Published: April 01, 2011

ACS Publications © 2011 American Chemical Society

particles with a size in submicrometer range (about 200 nm; Figure S6, Supporting Information) in sample **6** was distinct from all the other samples. In the presence of an excess amount of solvent, the monomers were cross-linked to form polymeric nuclei which grow gradually to form fairly isolated microporous polymer nano- or submicro-particles. The functional group in the monomer (e.g., phenolic hydroxy groups) can also affect the particle size and morphology. However, in the presence of a limited amount of solvent (DCE, 1 mL) continuous monolithic networks were formed[3c] (Figure S7, see Supporting Information for experimental details).

Scheme 1. Scheme Showing the Synthetic Pathway to the Network Structure[a]

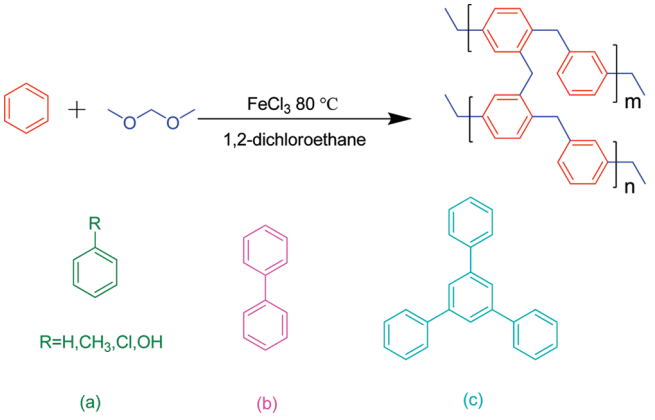

[a] Structures a–c are molecular structures of building blocks for the network.

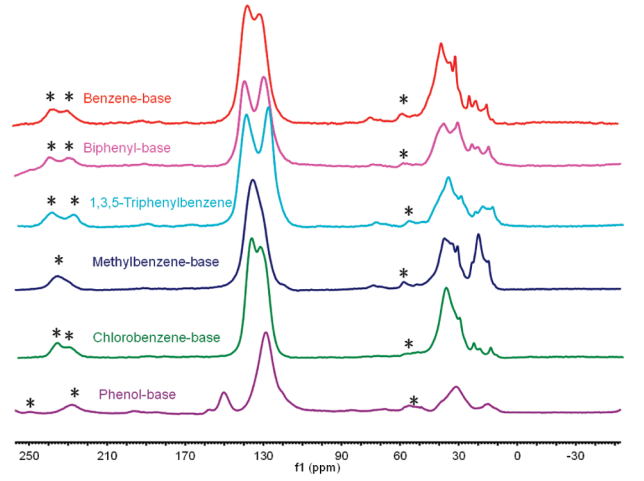

Figure 1. Cross-polarization (CP) ^{13}C MAS natural abundance NMR spectrum of samples. Asterisks denote spinning sidebands.

The successful growth of a microporous network, as well as high conversion of the available functional groups, were confirmed by Fourier transform infrared (FTIR) spectroscopy, ^{13}C cross-polarization magic-angle spinning (CP/MAS) NMR and elemental analysis (EA). In the FTIR spectrum of all samples (Figures S8–S13, Supporting Information), peaks near 1600, 1500, and 1450 cm^{-1} were attributed to aromatic ring skeleton vibrations which were consistent with the structure of monomers. The ^{13}C CP/MAS NMR of all samples (Figures 1 and S14–S19, Supporting Information) showed resonance peaks near 137 and 130 ppm due to substituted aromatic carbon and non-substituted aromatic carbon respectively, and the resonance peaks near 36 ppm due to carbon in methylene linker formed after Friedel–Crafts reaction (the resonance peaks of different samples showed a little variation according to the nature of functional groups and the knitting degree). The network based on methylbenzene showed resonance peaks at 22 ppm which can be assigned to methyl carbon connected to the benzene ring. The chlorine content of sample **5** was found to be 26.38% which confirmed that it incorporated by the chlorobenzene monomers. The network based on phenol possessed resonance peaks at 150 ppm due to aromatic carbons linked with phenolic hydroxyl group.

The porous properties of the samples were analyzed by nitrogen sorption analysis. Table 1 summarizes the characterization data such as surface area and the pore volume, and Table 2 summarizes the gas uptake for the various samples. The highest BET surface area (1391 m^2/g) was obtained for the benzene-based network. As shown in Figure 2a, the adsorption isotherms of all samples indicated a steep nitrogen gas uptake at low relative pressure ($P/P_0 < 0.001$), thus reflecting abundant micropore structure.[19] Figure 2b demonstrated that the different monomers led to different pore structure and chemical functionality in the resulting porous materials, and Figure 3 showed the distinct gas adsorption properties of these samples. Nitrogen adsorption and

Table 1. Composition and Porosity of the Samples

no.	monomer	FDA[a]	S_{BET}[b] (m^2/g)	S_L[c] (m^2/g)	PV[d] (cm^3/g)	MPV[e] (cm^3/g)
1	benzene	3	1391	1905	2.42	0.48
1A	benzene	2	1270	1749	1.67	0.43
1B	benzene	1.25	897	1232	0.7	0.31
2	biphenyl	6	815	1292	0.46	0.33
2A	biphenyl	2	397	536	0.15	0.26
2B	biphenyl	1.25	195	265	0.07	0.21
3	1,3,5-triphenylbenzene	6	1059	1424	0.71	0.44
4	methylbenzene	2	826	1117	0.53	0.31
5	chlorobenzene	3	438	596	0.36	0.16
6	phenol	2	400	532	0.21	0.16

[a] Molar ratio with respect to monomer. [b] Surface area calculated from nitrogen adsorption isotherms at 77.3 K using BET equation. [c] Surface area calculated from nitrogen adsorption isotherms at 77.3 K using Langmuir equation. [d] Pore volume calculated from nitrogen isotherm at $P/P_0 = 0.995$, 77.3 K. [e] Micropore volume calculated from the nitrogen isotherm at $P/P_0 = 0.050$.

dx.doi.org/10.1021/ma200630s |*Macromolecules* 2011, 44, 2410–2414

Table 2. H_2 Gas Adsorption and CO_2 Gas Adsorption of the Samples

no.	monomer	FDA[a]	H_2 uptake[b] wt % (mmol/g)	CO_2 uptake[c] wt % (mmol/g)
1	benzene	3	1.45 (7.25)	13.5 (3.07)
1A	benzene	2	1.32 (6.60)	12.2 (2.78)
1B	benzene	1.25	1.01 (5.05)	9.0 (2.04)
2	biphenyl	6	1.34 (6.70)	13.8 (3.14)
2A	biphenyl	2	0.72 (3.60)	6.9 (1.57)
2B	biphenyl	1.25	0.51 (2.55)	4.9 (1.11)
3	1,3,5-triphenylbenzene	6	1.58 (7.90)	15.9 (3.61)
4	methylbenzene	2	1.05 (5.25)	9.5 (2.16)
5	chlorobenzene	3	0.64 (3.20)	5.5 (1.25)
6	phenol	2	1.07 (5.35)	9.4 (2.14)

[a] Molar ratio with respect to monomer. [b] H_2 uptake determined volumetrically using a Micromeritics ASAP 2020 M analyzer at 1.13 bar and 77.3 K. [c] CO_2 uptake determined volumetrically using a Micromeritics ASAP 2020 M analyzer at 1.00 bar and 273.15 K.

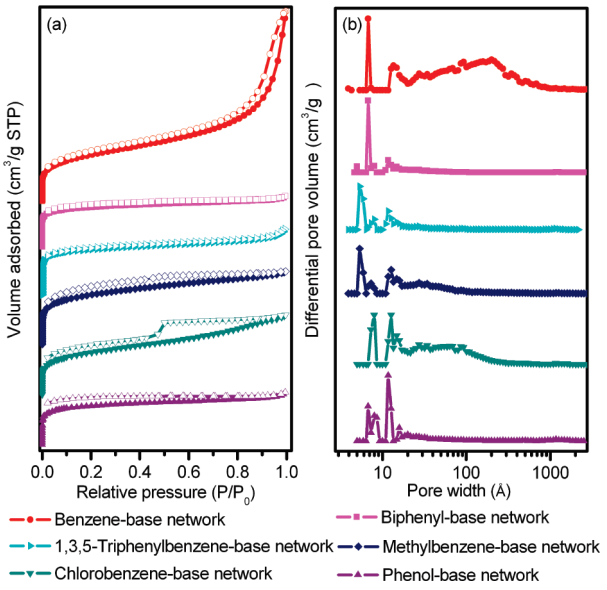

Figure 2. Nitrogen sorption isotherms at 77.3 K (a) and pore distribution of pore size distributions calculated using DFT methods (slit pore models, differential pore volumes. pore width (b) of samples.

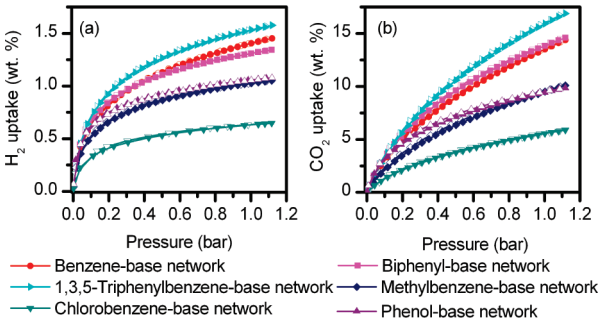

Figure 3. Volumetric H_2 adsorption isotherms and desorption isotherms up to 1.13 bar at 77.3 K (a) and volumetric CO_2 adsorption isotherms and desorption isotherms up to 1.13 bar at 273.15 K (b) of samples.

desorption isotherms of sample **1** (benzene-based) showed a slight hysteresis loop implying a spot of mesopore and exhibit a sharp rise at medium and high pressure region ($P/P_0 = 0.8-1.0$) indicating the presence of macropores in these materials.[19] The pore size distribution also confirmed the presence of such heterogeneous porous structure. Nitrogen adsorption and desorption isotherms of sample **2** (biphenyl-based) with flat course in the intermediate section was a typical type I according to the IUPAC classification[19] and there were no peaks at region over 2 nm in pore size distribution; hence, sample **2** possessed a pure microporous structure. Sample **3** (1,3,5-triphenylbenzene-based) was ultra microporous (pore size less than 0.7 nm) according to the pore size distribution consistent with its high H_2 uptake (77.3 K, 1.13 bar, 1.58 wt %, 7.90 mmol/g) and CO_2 uptake (273.15 K, 1.00 bar, 15.9 wt %, 3.61 mmol/g). The adsorption capacities for CO_2 are higher than most materials reported so far.[20] In comparison to the other samples, sample **4** (methylbenzene-based) exhibited low pressure hysteresis extending to the lowest attainable pressures, this phenomenon is associated with the irreversible uptake of gas molecules in the pores (or through pore entrances) of about the same width as that of the N_2 molecule (thermal transition hard-sphere diameters, d = 3.860 Å).[19] Sample **4** possessed some ultra micropores smaller than those for sample **3**, and also showed totally reversible H_2 (d = 2.970 Å) and CO_2 (d = 3.604 Å) isotherms, consistent with this conclusion. Comparing the pore size distribution of sample **1** and sample **4**, the $-CH_3$ group seemed responsible for pore volume difference resulting in the formation of ultra micropores in sample **4**. Alternatively, different connectivity in the networks might rationalize this difference. Nitrogen adsorption and desorption isotherms with evident hysteresis loop in steep region at P/P_0 = 0.42 implied mesopores in sample **5**.[19] This may be due to the lower Friedel−Crafts reactivity for this monomer which resulted in less $-CH_2-$ bridges being formed between benzene rings (Indeed ratios of C and H are lower than other samples which can support this conclusion). For sample **6**, although the BET surface area (400 m^2/g) is much lower than sample **4** (826 m^2/g), the H_2 and CO_2 adsorption properties were almost same. This may result from enhanced interactions with the phenolic hydroxyl group with the gas molecular,[19] or alternatively it may be an effect of pore size. Additionally, via adjusting the external cross-linker ratio, the surface area and pore volume also can be controlled. Comparing the sample set **1**, **1A**, **1B** and sample set **2**, **2A**, **2B** (Table 1 and 2) the surface area, pore volume, micropore volume, and gas adsorption properties are enhanced with increasing the cross-linker ratio.

Atomistic simulation[21] results (details described in Supporting Information) of a benzene-based network, a biphenyl-based network and a 1,3,5-triphenylbenzene-based network were

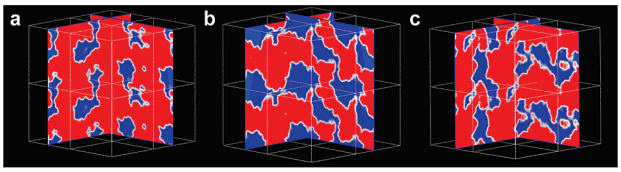

Figure 4. 2-Dimensional "slices" through the simulated pore structure of a benzene-based network (a), a biphenyl-based network (b) and a 1,3,5-triphenylbenzene-based network (c). The occupied and unoccupied volume is shown in red and blue, respectively.

consistent with experimental data. The Connolly surface area[22] (2359, 2035, and 2016 m^2/g for these three materials respectively) were found to follow the same trend as the Langmuir surface area (1905, 1292, and 1424 m^2/g for these three materials respectively). A two-dimensional "slice" through the simulated pore structure (Figure 4 and Figures S20c, S21c, and S22c, Supporting Information) simulated the pore micropore dimensions of these three samples quite well; the majority of the pore channels in width were 3−20 Å for benzene, 3−12 Å for biphenyl, 3−10 Å for 1,3,5-triphenylbenzene-based networks. This model simulated only microporosity in the material and did not account for the meso- or macroporosity; as mesopores in samples (e.g., benzene-based network) possessed the dimensions that were larger than those of the simulation cell (about 3.3 nm) as shown in pore size distributions (Figure 2b).

No changes in properties for any of the samples were observed upon exposure of the insoluble powders to humidity or to acidic or alkaline conditions. The samples also exhibited high thermal stability as evident by thermogravimetric analysis (T_{dec} > 400 °C, Figure S23, Supporting Information).

In summary, we report here a novel and general synthetic strategy for the design and synthesis of microporous polymers based on various rigid aromatic building blocks, including nonhalogenated monomer feedstocks.[21a] There are several outstanding characteristics of this strategy: (I) the range of possible structural building block is extensive (only a few possible examples are demonstrated here), and hence this method is versatile and flexible; (II) the mild synthesis conditions and the cheap reagents should allow economical and larger-scale production of such materials; (III) it has been demonstrated that the method can lead to materials with high surface area, abundant micropore structure and/or various functional groups;[23] (IV) different structural building blocks and adjustable cross-linker ratio can give rise to diverse pore structures and, potentially, unique properties for certain applications. We are now trying to apply this strategy to develop new materials by 'knitting' aromatic heterocyclic compounds (e.g., thiophene) or fused aromatic ring monomers (e.g., coronene) for selective gas storage applications because these compounds are known to possess better affinities with certain gas molecules. Knitting performed large conjugated aromatic rings (e.g., graphene) or conjugated macromolecular chains (e.g., polythiophene) to obtain porous materials with optical, electrical, or magnetically properties is also a possibility. Lastly, knitting small aromatic molecular catalyst may lead to high surface area materials for heterogeneous catalysis applications.[24]

■ ASSOCIATED CONTENT

Ⓢ Supporting Information. Experimental details, atomistic simulation details, SEM and TEM images, a photgraph of the monolith, Fourier transform infrared spectroscopy, ^{13}C cross-polarization magic-angle spinning (CP/MAS) NMR, simulated networks, elemental analysis and physical properties of the samples, and thermogravimetric analysis. This material is available free of charge via the Internet at http://pubs.acs.org.

■ AUTHOR INFORMATION

Corresponding Author

*E-mail: bien.tan@mail.hust.edu.cn.

■ ACKNOWLEDGMENT

We thank Prof. Andrew I. Cooper for fruitful discussions. We also thank the Analysis and Testing Center, Huazhong University of Science and Technology, for characterization assistance. This work was financially supported by the program for New Century Excellent Talents in University (NCET-10-0389) and National Natural Science Foundation of China (No. 50973037).

■ REFERENCES

(1) (a) McKeown, N. B.; Budd, P. M. *Chem. Soc. Rev.* **2006**, *35*, 675–683. (b) Li, B.; Su, F.; Luo, H.-K.; Liang, L.; Tan, B. *Microporous Mesoporous Mater.* **2011**, *138*, 207–214.

(2) (a) Du, X.; Sun, Y.; Tan, B.; Teng, Q.; Yao, X.; Su, C.; Wang, W. *Chem. Commun.* **2010**, *46*, 970–972. (b) Dang, D.; Wu, P.; He, C.; Xie, Z.; Duan, C. *J. Am. Chem. Soc.* **2010**, *132*, 14321–14323.

(3) (a) Furukawa, H.; Yaghi, O. M. *J. Am. Chem. Soc.* **2009**, *131*, 8875–8883. (b) McKeown, N. B.; Gahnem, B.; Msayib, K. J.; Budd, P. M.; Tattershall, C. E.; Mahmood, K.; Tan, S.; Book, D.; Langmi, H. W.; Walton, A. *Angew. Chem., Int. Ed.* **2006**, *118*, 1836–1839. (c) Wood, C. D.; Tan, B.; Trewin, A.; Su, F.; Rosseinsky, M. J.; Bradshaw, D.; Sun, Y.; Zhou, L.; Cooper, A. I. *Adv. Mater.* **2008**, *20*, 1916–1921. (d) Li, B.; Huang, X.; Liang, L.; Tan, B. *J. Mater. Chem.* **2010**, *20*, 7444–7450. (e) Holst, J. R.; Cooper, A. I. *Adv. Mater.* **2010**, *22*, 5212–5216.

(4) Ferey, G.; Mellot-Draznieks, C.; Serre, C.; Millange, F.; Dutour, J.; Surble, S.; Margiolaki, I. *Science* **2005**, *309*, 2040–2042.

(5) (a) Cote, A. P.; Benin, A. I.; Ockwig, N. W.; O'Keeffe, M.; Matzger, A. J.; Yaghi, O. M. *Science* **2005**, *310*, 1166–1170. (b) El-Kaderi, H. M.; Hunt, J. R.; Mendoza-Cortes, J. L.; Cote, A. P.; Taylor, R. E.; O'Keeffe, M.; Yaghi, O. M. *Science* **2007**, *316*, 268–272.

(6) Tozawa, T.; Jones, J. T. A.; Swamy, S. I.; Jiang, S.; Adams, D. J.; Shakespeare, S.; Clowes, R.; Bradshaw, D.; Hasell, T.; Chong, S. Y.; Tang, C.; Thompson, S.; Parker, J.; Trewin, A.; Bacsa, J.; Slawin, A. M. Z.; Steiner, A.; Cooper, A. I. *Nat. Mater.* **2009**, *8*, 973–978.

(7) Jiang, J.-X.; Cooper, A. Microporous Organic Polymers: Design, Synthesis, and Function. In *Functional Metal-Organic Frameworks: Gas Storage, Separation and Catalysis*, Schröder, M., Ed. Springer: Berlin and Heidelberg, Germany: 2010; Vol. 293, pp 1−33.

(8) Davankov, V. A.; Rogozhin, S. V.; Tsyurupa, M. P. 3,729,457, 1971.

(9) (a) Ahn, J. H.; Jang, J. E.; Oh, C. G.; Ihm, S. K.; Cortez, J.; Sherrington, D. C. *Macromolecules* **2006**, *39*, 627–632. (b) Macintyre, F. S.; Sherrington, D. C.; Tetley, L. *Macromolecules* **2006**, *39*, 5381–5384. (c) Tsyurupa, M. P.; Davankov, V. A. *React. Funct. Polym.* **2006**, *66*, 768–779.

(10) (a) Germain, J.; Svec, F.; Frechet, J. M. J. *Chem. Mater.* **2008**, *20*, 7069–7076. (b) Germain, J.; Frechet, J. M. J.; Svec, F. *Chem. Commun.* **2009**, 1526–1528.

(11) (a) Jiang, J. X.; Su, F.; Trewin, A.; Wood, C. D.; Niu, H.; Jones, J. T. A.; Khimyak, Y. Z.; Cooper, A. I. *J. Am. Chem. Soc.* **2008**, *130*, 7710–7720. (b) Schmidt, J.; Werner, M.; Thomas, A. *Macromolecules* **2009**, *42*, 4426–4429.

(12) Ben, T.; Ren, H.; Ma, S.; Cao, D.; Lan, J.; Jing, X.; Wang, W.; Xu, J.; Deng, F.; Simmons, J.; Qiu, S.; Zhu, G. *Angew. Chem., Int. Ed.* **2009**, *48*, 9457–9460.

(13) Yuan, S. W.; Dorney, B.; White, D.; Kirklin, S.; Zapol, P.; Yu, L. P.; Liu, D. J. *Chem. Commun.* **2010**, *46*, 4547–4549.
(14) Kuhn, P.; Antonietti, M.; Thomas, A. *Angew. Chem., Int. Ed.* **2008**, *47*, 3450–3453.
(15) (a) Weber, J.; Antonietti, M.; Thomas, A. *Macromolecules* **2008**, *41*, 2880–2885. (b) Pandey, P.; Katsoulidis, A. P.; Eryazici, I.; Wu, Y.; Kanatzidis, M. G.; Nguyen, S. T. *Chem. Mater.* **2010**, *22*, 4974–4979. (c) Uribe-Romo, F. J.; Hunt, J. R.; Furukawa, H.; Klöck, C.; O'Keeffe, M.; Yaghi,, O. M., *J. Am. Chem. Soc.* **2009**, *131*, 4570–4571.
(16) (a) Holst, J. R.; Stöckel, E.; Adams, D. J.; Cooper, A. I. *Macromolecules* **2010**, *43*, 8531–8538. (b) Pandey, P.; Farha, O. K.; Spokoyny, A. M.; Mirkin, C. A.; Kanatzidis, M. G.; Hupp, J. T.; Nguyen, S. T. *J. Mater. Chem.* **2011**, *21*, 1700–1703.
(17) Yuan, S. W.; Kirklin, S.; Dorney, B.; Liu, D. J.; Yu, L. P. *Macromolecules* **2009**, *42*, 1554–1559.
(18) Jiang, J.-X.; Laybourn, A.; Clowes, R.; Khimyak, Y. Z.; Bacsa, J.; Higgins, S. J.; Adams, D. J.; Cooper, A. I. *Macromolecules* **2010**, *43*, 7577–7582.
(19) Sing, K. S. W.; Everett, D. H.; Haul, R. A. W.; Moscou, L.; Pierotti, R. A.; Rouquerol, J.; Siemieniewska, T. *Pure Appl. Chem.* **1985**, *57*, 603–619.
(20) Hedin, N.; Chen, L.; Laaksonen, A. *Nanoscale* **2010**, *2*, 1819–1841.
(21) (a) Wood, C. D.; Tan, B.; Trewin, A.; Niu, H. J.; Bradshaw, D.; Rosseinsky, M. J.; Khimyak, Y. Z.; Campbell, N. L.; Kirk, R.; Stockel, E.; Cooper, A. I. *Chem. Mater.* **2007**, *19*, 2034–2048. (b) Trewin, A.; Willock, D. J.; Cooper, A. I. *J. Phys. Chem. C* **2008**, *112*, 20549–20559.
(22) Connolly, M. *Science* **1983**, *221*, 709–713.
(23) Dawson, R.; Laybourn, A.; Clowes, R.; Khimyak, Y. Z.; Adams, D. J.; Cooper, A. I. *Macromolecules* **2009**, *42*, 8809–8816.
(24) Jiang, J.-X.; Wang, C.; Laybourn, A.; Hasell, T.; Clowes, R.; Khimyak, Y. Z.; Xiao, J.; Higgins, S. J.; Adams, D. J.; Cooper, A. I. *Angew. Chem., Int. Ed.* **2011**, *50*, 1072–1075.